bioRxiv preprint doi: https://doi.org/10.1101/681221; this version posted January 28, 2020. The copyright holder for this preprint (which was not certified by peer review) is the author/funder, who has granted bioRxiv a license to display the preprint in perpetuity. It is made available under aCC-BY-NC-ND 4.0 International license.

Maturation of cortical microstructure and cognitive development in childhood and adolescence: a T1w/T2w ratio MRI study

Linn B. Norbom[a,b,c*], Jaroslav Rokicki[a,d], Dag Alnæs[a], Tobias Kaufmann[a], Nhat Trung Doan[a], Ole A. Andreassen[a], Lars T. Westlye[a,d], Christian K. Tamnes[a,b,c]

[a] NORMENT, Division of Mental Health and Addiction, Oslo University Hospital & Institute of Clinical Medicine, University of Oslo, Norway

[b] PROMENTA Research Center, Department of Psychology, University of Oslo, Norway

[c] Department of Psychiatric Research, Diakonhjemmet Hospital, Oslo, Norway

[d] Department of Psychology, University of Oslo, Norway

Corresponding authors P.O. box 1094 Blindern, 0317 Oslo, Norway.

*l.c.b.norbom@psykologi.uio.no

Running title: Maturation of cortical microstructure

Keywords: adolescence; brain development; children; cognition; myelination; signal intensity; T1w/T2w ratio

bioRxiv preprint doi: https://doi.org/10.1101/681221; this version posted January 28, 2020. The copyright holder for this preprint (which was not certified by peer review) is the author/funder, who has granted bioRxiv a license to display the preprint in perpetuity. It is made available under aCC-BY-NC-ND 4.0 International license.

Abstract

The restructuring and optimization of the cerebral cortex from early childhood and through adolescence is an essential feature of human brain development, underlying immense cognitive improvements. Beyond established morphometric cortical assessments, the T1w/T2w ratio quantifies partly separate biological processes, and might inform models of typical neurocognitive development and developmental psychopathology. In the present study, we computed vertex-wise T1w/T2w ratio across the cortical surface in 621 youths (3-21 years) sampled from the Pediatric Imaging, Neurocognition, and Genetics (PING) study and tested for associations with individual differences in age, sex, and both general and specific cognitive abilities. The results showed a near global linear age-related increase in T1w/T2w ratio across the brain surface, with a general posterior to anterior increasing gradient in association strength. Moreover, results indicated that boys in late adolescence had regionally higher T1w/T2w ratio as compared to girls. Across individuals, T1w/T2w ratio was negatively associated with general and several specific cognitive abilities mainly within anterior cortical regions. Our study indicates age-related differences in T1w/T2w ratio throughout childhood, adolescence and young adulthood, in line with the known protracted myelination of the cortex. Moreover, the study supports the relevance of the T1w/T2w ratio as a neuroimaging marker for cognitive development.

bioRxiv preprint doi: https://doi.org/10.1101/681221; this version posted January 28, 2020. The copyright holder for this preprint (which was not certified by peer review) is the author/funder, who has granted bioRxiv a license to display the preprint in perpetuity. It is made available under aCC-BY-NC-ND 4.0 International license.

Introduction

Childhood and adolescence is a time of extensive brain maturation and reorganization, shaped by multiple genetically based biological processes in dynamic interplay with the environment (Blakemore, 2012; Brown & Jernigan, 2012; Kremen et al., 2013; Lebel & Deoni, 2018). Magnetic resonance imaging (MRI) indicates that structural cortical development is characterized by widespread, but regionally variable and coordinated nonlinear decreases in volume and thickness, and early increases followed by smaller decreases in surface area (Amlien et al., 2016; Khundrakpam et al., 2019; Tamnes et al., 2017). This cortical maturation is mirrored by immense cognitive improvements from early childhood to young adulthood, with the development of basic functions such as sensorimotor processes preceding complex functions such as top-down control of behavior (Akshoomoff et al., 2014; Casey, Tottenham, Liston, & Durston, 2005). Detailed knowledge about cortical maturational patterns in youth is critical for models of normative neurocognitive development, and for serving as a blueprint for detecting neurodevelopmental deviations linked to maladjustment and psychopathology.

In addition to cortical morphometry, less explored measures of signal intensity variation in the T1-weighted (T1w) image may reflect additional and partly distinct neurobiological properties and processes (Andrews et al., 2017; Lewis, Evans, & Tohka, 2018; Lewis, Fonov, Collins, Evans, & Tohka, 2019; Norbom et al., 2019; Salat et al., 2009). Maturational and aging related cortical thinning have, for instance, been teased apart by their inverse relationships with cortical T1w intensity, which increases during development and declines in older aging (Westlye et al., 2010). More recently, T1w/T2w ratio has been suggested as a useful and possibly more specific measure of cortical microstructure (Glasser & Van Essen, 2011; Van Essen & Glasser, 2014). A handful of studies support the utility of T1w/T2w ratio for mapping global and regional maturational and aging related patterns

bioRxiv preprint doi: https://doi.org/10.1101/681221; this version posted January 28, 2020. The copyright holder for this preprint (which was not certified by peer review) is the author/funder, who has granted bioRxiv a license to display the preprint in perpetuity. It is made available under aCC-BY-NC-ND 4.0 International license.

(Grydeland et al., 2019; Grydeland, Walhovd, Tamnes, Westlye, & Fjell, 2013; Shafee, Buckner, & Fischl, 2015), and associations with cognitive performance in youth (Grydeland et al., 2013; Vandewouw, Young, Shroff, Taylor, & Sled, 2019) and adults (Grydeland, Westlye, Walhovd, & Fjell, 2016).

Although the underlying biology of the T1w/T2w ratio is controversial (Hagiwara et al., 2018; Ritchie, Pantazatos, & French, 2018; Uddin, Figley, Solar, Shatil, & Figley, 2019) and likely complex, the measure has been linked to differential myelination of the cerebral cortex (Ganzetti, Wenderoth, & Mantini, 2014; Glasser & Van Essen, 2011; Nakamura, Chen, Ontaneda, Fox, & Trapp, 2017). Intracortical myelination is a crucial feature of postnatal brain development, allowing for efficient signal transmission and structural support (Baumann & Pham-Dinh, 2001; Liu, Li, Zhu, Li, & Liu, 2019; Waxman & Bennett, 1972), and generally follows a posterior to anterior maturational pattern (Yakovlev & Lecours, 1967), with additional regional specificity (Deoni, Dean, Remer, Dirks, & O'Muircheartaigh, 2015; Nieuwenhuys, 2013; Ziegler et al., 2019). Cortical dysmyelination has also been linked to neurodevelopmental psychopathology (Bartzokis, 2005; Insel, 2010). Although T1w/T2w ratio shows promise for capturing distinct patterns of typical brain development, individual- and age-related differences have not been mapped in a large sample of children and/or adolescents, nor in relation to cognitive abilities.

To this end, we computed vertex-wise T1w/T2w ratio across the cortical surface in 621 youths (3-21 years) from the Pediatric Imaging, Neurocognition, and Genetics (PING) sample, and tested for associations between T1w/T2w ratio and age, sex and both general and specific cognitive abilities. We hypothesized that the T1w/T2w ratio would generally show a positive age association, putatively reflecting protracted intracortical myelination, but with regional variation. Next, given previous findings of limited sex differences in morphometric cortical development (Vijayakumar et al., 2016; Wierenga, Bos, van Rossenberg, & Crone,

bioRxiv preprint doi: https://doi.org/10.1101/681221; this version posted January 28, 2020. The copyright holder for this preprint (which was not certified by peer review) is the author/funder, who has granted bioRxiv a license to display the preprint in perpetuity. It is made available under aCC-BY-NC-ND 4.0 International license.

2019), we predicted that boys and girls would show similar age related associations with T1w/T2w ratio. Finally, we tested for associations between T1w/T2w ratio and general and specific cognitive abilities, and predicted a positive association, based on the direction of reported developmental T1w/T2w findings (Grydeland et al., 2019; Shafee et al., 2015).

Materials and Methods

Participants

The publicly available PING study database (http://ping.chd.ucsd.edu) consists of data from a large sample of typically developing children and adolescents aged 3-21 years, with standardized behavioral measures, whole genome genotyping, and multimodal imaging for a large subgroup (Jernigan et al., 2016). Fluent English speakers within the desired age range were recruited across the US through local postings and outreach facilities. Exclusion criteria included somatic illness, history of head trauma, contraindications for MRI, preterm birth, diagnosis of mental disorders (except ADHD), mental retardation, and severe illicit drug use by mother during pregnancy. Subjects 18 years and above provided written informed consent, while written parental informed consent was obtained for all other subjects, in addition to child assent for subjects aged 7-17 (Jernigan et al., 2016).

From 998 subjects with available MRI and demographic data, T2-weighted (T2w) data was missing or acquired at insufficient resolution (> 1.2mm voxel size in any direction) for 322 subjects. Of the remainder, we additionally excluded 55 subjects after stringent quality control (see below), yielding a final sample of 621 subjects (303 girls) aged 3.2-21.0 years (mean = 12.4, SD = 4.8). Ten of these subjects had missing cognitive data and were excluded from relevant analyses. See Table 1 for sample demographics.

MRI acquisition and processing

bioRxiv preprint doi: https://doi.org/10.1101/681221; this version posted January 28, 2020. The copyright holder for this preprint (which was not certified by peer review) is the author/funder, who has granted bioRxiv a license to display the preprint in perpetuity. It is made available under aCC-BY-NC-ND 4.0 International license.

Imaging data for our final sample was attained on 7 separate 3T scanners; 2 from GE medical systems (Signa HDx and Discovery MR750), and 5 from Siemens (TrioTim). The age-ranges were largely overlapping across scanners (Figure 1). To account for challenges associated with multisite imaging of children, an optimized imaging protocol was implemented across vendors and models to obtain similar contrast properties and image-derived quantitative measures (Jernigan et al., 2016). The protocol included a 3D T1w inversion prepared RF-spoiled gradient echo scan , and a 3D T2w variable flip angle fast spin echo scan (Jernigan et al., 2016), both acquired with prospective motion correction (PROMO) (White et al., 2010). Voxel sizes ranged from ≈ 0.9-1.2mm^3. See Supporting Information for additional acquisition parameters, and care and safety procedures implemented for scanning children.

Imaging processing was performed using the three step Human Connectome Project (HCP) pipeline as described elsewhere (Glasser et al., 2013). In short, the "PreFreeSurfer" stage produces an undistorted native structural volume space, aligns the T1w and T2w image, performs bias field correction calculated from the product of both images, and registers the native- to the common coordinate MNI space using a rigid 6 degrees of freedom transform, derived from a 12 degrees of freedom affine registration. Based on FreeSurfer version 6, the "FreeSurfer" stage performs volume segmentation, and cortical surface reconstructions, including the "white"- (grey/white matter boundary), and "pial"- (grey/cerebrospinal fluid (CSF) boundary) surface, and registers the surfaces to a common template (fsaverage). Due to some cases exhibiting large cortical thickness and T1w/T2w ratio discrepancies between the left and right hemisphere following the default pipeline, we removed a flag ("t2pial") within autorecon3, which when employed additionally uses the T2w sequence to reconstruct the pial surface. The "PostFreeSurfer" stage produces NIFTI volume- and GIFTI surface files, registers surfaces to the HCP standard mesh, and creates the final brain masks and T1w/T2w ratio maps (Glasser et al., 2013).

bioRxiv preprint doi: https://doi.org/10.1101/681221; this version posted January 28, 2020. The copyright holder for this preprint (which was not certified by peer review) is the author/funder, who has granted bioRxiv a license to display the preprint in perpetuity. It is made available under aCC-BY-NC-ND 4.0 International license.

T1w/T2w ratio maps

The creation of T1w/T2w ratio maps was based on methods described by Glasser and Van Essen (2011). A volume-to-surface mapping algorithm was applied to all voxel centers located within the cortical ribbon to achieve image division. For each vertex within the HCP pipeline surface "midthickness", ribbon voxels were selected within a cylinder centered on the vertex, orthogonal to the surface, and with a height and radius equal to the local cortical thickness. To remove voxels with significant blood vessel- and CSF partial voluming effects, voxels were excluded if the T1w/T2w value exceeds ±1 SD of all values within the cortical ribbon. The remaining ribbon voxels were then averaged following a Gaussian weighted function to produce a single value for each vertex, while the medial wall was assigned values of zero (Glasser & Van Essen, 2011). The final output includes standard and bias corrected non-smoothed and smoothed (Full width at half maximum = 4mm) maps.

Quality assessment of imaging data

We performed extensive quality assessment as multisite projects inevitably creates inconsistencies and since in-scanner head motion is more frequent in younger subjects. For subjects with both T1w and T2w data of sufficient resolution, all NIFTI images were processed through the automatic quality assessment pipeline MRIQC (Esteban et al., 2017). This program returns flagging of poor images as well as a numeric quality index based on measures of noise, spatial and tissue distribution, artifacts such as motion, and sharpness (Esteban et al., 2017). After visual inspection of flagged datasets by a single trained rater, subjects were either included, tagged for detailed re-assessment after T1w/T2w ratio map creation, or excluded due to poor image quality when there was no option to replace the image with another satisfactory run. The remaining subjects were subsequently processed through

bioRxiv preprint doi: https://doi.org/10.1101/681221; this version posted January 28, 2020. The copyright holder for this preprint (which was not certified by peer review) is the author/funder, who has granted bioRxiv a license to display the preprint in perpetuity. It is made available under aCC-BY-NC-ND 4.0 International license.

the HCP pipeline (Glasser et al., 2013). Finally, the same rater visually inspected all T1w/T2w ratio maps and excluded subjects with poor maps. See Supporting Information for in detail descriptions of quality assessments.

Cognitive assessment

All subjects completed the computerized NIH Toolbox Cognition Battery (Akshoomoff et al., 2014; Weintraub, Bauer, et al., 2013; Weintraub, Dikmen, et al., 2013) which includes seven different tasks, designed to measure eight diverse cognitive abilities, and is appropriate for use in children as young as 3 years of age (Table 2, and Supporting Information). Test order was standardized across participants, and eight sum scores were calculated as described elsewhere (Akshoomoff et al., 2014). Due to missing cognitive data on specific tests, we imputed 78 sum score values in total, from 63 subjects in R, using the "mice" package (Buuren & Groothuis-Oudshoorn, 2011), with the default of 5 multiple imputations, and choosing the first imputation. As expected, there were high correlations between all sum scores and age (Pearson's r ranging from 0.63 to 0.82), and we therefore residualized sum scores by linear and quadratic age by linear regression. Retrieving a single factor for general cognitive ability, conceptually similar to the IQ score, we then performed a principal component analysis (PCA) in R (https://www.r-project.org/) and the first factor, explaining 33.7% of the variance, was extracted and used as a measure of general cognitive ability. We changed the sign of the component so that higher factor loading would represent better performance. See Supporting Figure 1 for a bar plot of the percentage explained variance for each principal component, and Figure 2 for a correlation matrix between age, sex, general cognitive ability and individual cognitive sum scores.

Statistical analyses

bioRxiv preprint doi: https://doi.org/10.1101/681221; this version posted January 28, 2020. The copyright holder for this preprint (which was not certified by peer review) is the author/funder, who has granted bioRxiv a license to display the preprint in perpetuity. It is made available under aCC-BY-NC-ND 4.0 International license.

We used general linear models (GLM), as implemented in the Permutation Analysis of Linear Models (PALM) toolbox (Winkler, Ridgway, Webster, Smith, & Nichols, 2014), to test for linear and quadratic (defined as polynomial of degree 2) effects of age on vertex-wise T1w/T2w ratio, covarying for sex and scanner. Second, we tested for main effects of sex on vertex-wise T1w/T2w ratio, covarying for linear and quadratic age and scanner, and then for interaction effects between sex and age, with main effect of sex as an additional covariate. Third, we performed vertex-wise analyses to assess the effects of general cognitive ability, as well as each of the eight specific sum scores, all in separate models on vertex-wise T1w/T2w ratio, each time with sex, linear and quadratic age, sex*age and scanner as co-variates. Finally, we examined interaction effects between age and general cognitive ability on T1w/T2w ratio, with sex, linear and quadratic age, sex*age, general cognitive ability and scanner as co-variates. To assess statistical significance we used 10,000 permutations and family wise error (FWE) correction with threshold-free cluster enhancement (TFCE) (Smith & Nichols, 2009) corrected across each contrast (as PALM performs one tailed analyses) and a significance threshold of $p<0.05$, after correcting for both hemispheres.

To regionally summarize relevant vertex-wise results, we averaged our t-statistic surface maps within 34 regions of interest (ROIs) for both the left and right hemisphere. ROIs were defined by Freesurfer's fsaverage Desikan-Killiany Atlas parcellation (Desikan et al., 2006; Fischl et al., 2004) which was converted to GIFTI format and mapped to the HCP common mesh. To further visualize relevant PALM results, we used individual parcellations and locally weighted scatterplot smoothing (loess) and ggplot2 (Wickham, 2009) in R (https://www.r-project.org/).

Results

T1w/T2w mean ratio map

bioRxiv preprint doi: https://doi.org/10.1101/681221; this version posted January 28, 2020. The copyright holder for this preprint (which was not certified by peer review) is the author/funder, who has granted bioRxiv a license to display the preprint in perpetuity. It is made available under aCC-BY-NC-ND 4.0 International license.

Figure 3 shows the mean T1w/T2w ratio map across all subjects. Briefly, the anatomical signal distribution corresponded well with previous T1w/T2w maps (Glasser & Van Essen, 2011), showing a specific regional pattern in which sensorimotor regions, such as pre-and post-central gyri and visual cortex, showed relatively higher T1w/T2w ratio, while the frontal lobe and temporal pole showed relatively lower T1w/T2w ratio.

Associations between T1w/T2w ratio and age

Permutation testing revealed a near global positive association between linear age and T1w/T2w ratio, indicating higher ratio in widespread regions with higher age when controlling for sex (Figure 4). There was a general posterior to anterior increasing gradient in association strength, with highest mean t-statistics found in precentral, caudal middle frontal, pars triangularis, and postcentral regions within the left hemisphere, and rostal middle frontal, caudal middle frontal, precentral, and paracentral regions within the right hemisphere (Table 3). Sub-regions within the medial occipital lobe and minor medial parietal and frontal regions did not show significant age associations.

There were no statistically significant associations between T1w/T2w ratio and quadratic age, controlling for linear age and sex. Corresponding with our vertex-wise results, ROI-based plots with non-parametric loess curves showed steady increases of T1w/T2w ratio with higher age (Figure 5).

Associations between T1w/T2w ratio and sex

Permutation testing revealed no statistically significant main effect of sex on vertex-wise T1w/T2w ratio. There were, however, significant positive interaction effects between sex and age (Figure 6). Effects were more widespread in the left compared to the right hemisphere with highest mean t-statistics found in pars orbitalis, rostral middle frontal, pars triangularis

bioRxiv preprint doi: https://doi.org/10.1101/681221; this version posted January 28, 2020. The copyright holder for this preprint (which was not certified by peer review) is the author/funder, who has granted bioRxiv a license to display the preprint in perpetuity. It is made available under aCC-BY-NC-ND 4.0 International license.

and frontal pole in the left hemisphere, and frontal pole, superior frontal, rostral middle frontal and rostral anterior cingulate in the right hemisphere (Table 3). Corresponding with our vertex-wise results, frontal ROI-based plots showed a pattern where boys within the age-range of approximately 15-21 years had relatively higher T1w/T2w ratio than girls (Figure 7).

Associations between T1w/T2w ratio and cognition

Permutation testing revealed a negative relationship between T1w/T2w ratio and general cognitive ability in the frontal lobe extending into left temporal pole and right parietal regions, with more widespread associations in left compared to the right hemisphere (Figure 8). This indicates that lower T1w/T2w ratio was associated with better cognitive performance. Strongest negative associations were found in pars orbitalis, pars triangularis, temporal pole and caudal middle frontal regions in the left hemisphere, and pars orbitalis, inferior parietal, precentral and supra marginal regions in the right hemisphere (Table 3).

Permutation testing revealed no significant interaction effects between general cognitive ability and age on T1w/T2w ratio. Corresponding with our vertex-wise results, ROI-based plots indicated that higher general cognitive ability was associated with regionally lower T1w/T2w ratio across the age-range (Figure 9). Moreover, 5 specific cognitive sum scores yielded regional negative associations with T1wT2w ratio, with varying cluster extension after correction across hemispheres, largely overlapping with the regions reported for general cognitive ability (Figure 10). Inhibition and attention showed small clusters within the left hemisphere, with inhibition covering precentral and postcentral sub regions, and attention covering the postcentral region only. While vocabulary only showed associations in small frontal clusters within the left hemisphere, the vertex-wise pattern for reading was widespread and highly similar to the pattern found for general cognitive ability, with frontal associations stronger in the left as compared to the right hemisphere. Finally, working

bioRxiv preprint doi: https://doi.org/10.1101/681221; this version posted January 28, 2020. The copyright holder for this preprint (which was not certified by peer review) is the author/funder, who has granted bioRxiv a license to display the preprint in perpetuity. It is made available under aCC-BY-NC-ND 4.0 International license.

memory showed regional associations within right hemisphere only, mainly in parietal regions, covering highly similar areas as general cognitive ability. There were no significant associations between T1w/T2w ratio and cognitive flexibility, episodic memory and processing speed.

Discussion

The cerebral cortex is the center for most of our evolutionarily unique cognitive abilities (Geschwind & Rakic, 2013), and its maturation is therefore an essential part of human brain development, underpinning major environmental adaptations and vast cognitive improvements (Casey et al., 2005). In a large sample of youths aged 3-21 years we found a global age-related increase of T1w/T2w ratio across the brain surface, with some regional and sex related variation. Intriguingly, across individuals, T1w/T2w ratio was inversely associated with general and several specific cognitive abilities, mainly in anterior cortical regions.

The first goal of the present study was to investigate associations between T1w/T2w ratio and age. As hypothesized, we found a near global positive association, with a continuous age-related increase of T1w/T2w ratio from early childhood and into young adulthood. Our results converge with the few prior studies on T1w/T2w ratio in children, adolescents and young adults (Grydeland et al., 2013; Shafee et al., 2015). Grydeland et al. (2013) reported that for their youngest age group, consisting of 8 to 19 year old subjects, there was a positive linear association between T1w/T2w ratio and age across large portions of the cerebral cortex, with strongest association in posterior frontal, parietal, and temporal cortices. We too found our strongest associations in posterior frontal regions extending into parietal regions. In contrast to the present results, Grydeland et al. did not find age-associations within parts of anterior frontal and insular cortices, but this discrepancy could be due to greater sample size and the inclusion of younger children in the current study.

bioRxiv preprint doi: https://doi.org/10.1101/681221; this version posted January 28, 2020. The copyright holder for this preprint (which was not certified by peer review) is the author/funder, who has granted bioRxiv a license to display the preprint in perpetuity. It is made available under aCC-BY-NC-ND 4.0 International license.

Our analyses revealed no significant main effects of sex on T1w/T2w ratio, but a positive age by sex interaction indicated that boys in late adolescence had relatively higher T1w/T2w ratio than girls in the frontal lobe and parts of parietal lobe. No previous studies have to our knowledge specifically investigated the relationship between T1w/T2w ratio and sex, but several studies have tested for sex differences in cortical morphometry and morphometric development. Although there are inconsistencies in this literature, recent longitudinal results indicate larger cortical volumes and areas in boys, but few differences in cortical thickness, and limited sex differences in the estimated rates of cortical morphometric development (Vijayakumar et al., 2016; Wierenga et al., 2019). A recent study investigating a longitudinal sample of 14 to 24 year old youths, using magnetization transfer (MT), an imaging measure linked to myelination, reported main effects of sex, with females having regionally higher MT than males (Ziegler et al., 2019). Less optimal cross sectional analyses of the same data, yielded a similar sex-age interactional pattern to the one reported in the current study, within right angular gyrus. Therefore, future longitudinal studies on T1w/T2w ratio are needed for more direct investigations.

Few previous studies have explored the behavioral and cognitive relevance of T1w/T2w ratio during development. We found a negative association between T1w/T2w ratio and general cognitive ability, mainly in anterior regions. We also found corresponding associations regarding both direction and cumulative regional extension between T1w/T2w ratio and the specific cognitive abilities: inhibition, attention, reading, vocabulary and working memory. We did not find an interaction between cognitive ability and age on T1w/T2w ratio. Intriguingly, this indicates that beyond developmental improvements, children and adolescents with high general- and specific cognitive performance have regionally lower T1w/T2w ratio especially within the frontal lobe. Considering the positive T1w/T2w ratio - age association, this result is surprising. However, it does converge with

bioRxiv preprint doi: https://doi.org/10.1101/681221; this version posted January 28, 2020. The copyright holder for this preprint (which was not certified by peer review) is the author/funder, who has granted bioRxiv a license to display the preprint in perpetuity. It is made available under aCC-BY-NC-ND 4.0 International license.

several studies reporting negative or otherwise unexpected direction of associations between diffusion metrics and cognitive skills in children (Dougherty et al., 2007; Huber, Henriques, Owen, Rokem, & Yeatman, 2019; Travis, Adams, Kovachy, Ben-Shachar, & Feldman, 2017). Our results also mostly concord with the very limited prior literature on T1w/T2w ratio and cognition in youth. Grydeland et al. (2013) investigated the relationship between T1w/T2w ratio and performance variability in response time in youths and adults. Although the general conclusion, based on the combined lifespan sample, was that higher T1w/T2w ratio was associated with greater performance stability, the opposite relationship was reported for the young subgroup of 8 to 19 year old subjects in clusters within occipital and parietal regions. However, a recent study by Vandewouw et al. (2019) found lower T1w/T2w ratio within occipital, parietal and subcortical regions in a small group of four year old preterm children as compared to children born full term. Across the two groups, they also found positive associations between T1w/T2w ratio in parietal lobes and intelligence, and expressive and receptive language ability.

The biological underpinnings of the T1w/T2w ratio is debated and likely complex. On the one hand, intracortical myelin content inversely co-varies with the T1w and T2w signal intensity (Glasser & Van Essen, 2011), through differences in lipids (Koenig, 1991), water concentration (Miot-Noirault, Barantin, Akoka, & Le Pape, 1997), and iron which in the cortex is strongly co-located with myelin (Fukunaga et al., 2010). The T1w- to T2w division also mathematically cancels most scanner related intensity biases, while increasing contrast (Glasser & Van Essen, 2011), and T1w/T2w ratio concurs with post mortem data (Nakamura et al., 2017). On the other hand, recent attempts have not revealed close links between T1w/T2w ratio and either myelin-related genes or more established myelin measures (Hagiwara et al., 2018; Ritchie et al., 2018; Uddin et al., 2019), demonstrating that it is not a straightforward myelin proxy. Nevertheless, our T1w/T2w ratio - age results are in line with

bioRxiv preprint doi: https://doi.org/10.1101/681221; this version posted January 28, 2020. The copyright holder for this preprint (which was not certified by peer review) is the author/funder, who has granted bioRxiv a license to display the preprint in perpetuity. It is made available under aCC-BY-NC-ND 4.0 International license.

the known protracted maturational timing and directional pattern of intracortical myelination (Miller et al., 2012; Yakovlev & Lecours, 1967). The observed negative associations between T1w/T2w ratio and cognition are less intuitive if interpreted through a cortical myelin perspective. One could speculate that having excess levels of cortical myelin beyond a certain normative developmental range, is disadvantageous as myelin contains factors associated with inhibition of neurite growth. Excess myelin might consequently foster a permanent inhibitory environment for synapse formation and lower neuronal plasticity (Snaidero & Simons, 2017). Another possibility, as suggested by several diffusion studies (Dougherty et al., 2007; Huber et al., 2019; Travis et al., 2017) is that, in children, other tissue factors besides myelin content may account for variations in cognitive skills. As the frontal lobe contains low myelin content and shows protracted maturation, there might be distinct tissue properties underlying our cognitive- and age related findings.

We did not find associations between T1w/T2w ratio and age in sub regions of medial occipital lobe and minor medial parietal and frontal regions, probably due to removal of the t2pial flag during the HCP pipeline (see Supporting Information). Other study limitations include the cross-sectional design, which is a sub-optimal and indirect way to investigate maturation and development. Moreover, imaging data was attained on several different scanners, and although statistically controlled for in all analyses, this will still most likely confound variables of interest.

To conclude, our results indicated that cortical T1w/T2w ratio almost globally increases from early childhood until young adulthood, corresponding with established maturational patterns of intracortical myelination. We also found that T1w/T2w ratio was inversely associated with measures of both general and several specific cognitive abilities, especially in anterior cortical regions. Future studies, preferably longitudinal, are needed to

bioRxiv preprint doi: https://doi.org/10.1101/681221; this version posted January 28, 2020. The copyright holder for this preprint (which was not certified by peer review) is the author/funder, who has granted bioRxiv a license to display the preprint in perpetuity. It is made available under aCC-BY-NC-ND 4.0 International license.

validate the robustness of these developmental patterns and links with individual cognitive differences and developmental psychopathology.

Acknowledgments and disclosures

This work was supported by the Department of Psychology, University of Oslo (LBN and CKT), the Research Council of Norway (223273, 249795, 230345), the South-Eastern Norway Regional Health Authority (2019069, 2014097, 2016083), and the European Commission's 7th Framework Programme (602450, IMAGEMEND). Data collection and sharing was funded by the Pediatric Imaging, Neurocognition and Genetics Study (PING) (National Institutes of Health Grant RC2DA029475). PING is funded by the National Institute on Drug Abuse and the Eunice Kennedy Shriver National Institute of Child Health & Human Development. PING data are disseminated by the PING Coordinating Center at the Center for Human Development, University of California, San Diego. Data were also in part provided by the Human Connectome Project, WU-Minn Consortium (Principal Investigators: David Van Essen and Kamil Ugurbil; 1U54MH091657) funded by the 16 NIH Institutes and Centers that support the NIH Blueprint for Neuroscience Research; and by the McDonnell Center for Systems Neuroscience at Washington University. A preprint is published on bioRxiv.org. The authors report no biomedical financial interests or potential conflicts of interest. The data that support the findings of this study are available on request from the corresponding author.

bioRxiv preprint doi: https://doi.org/10.1101/681221; this version posted January 28, 2020. The copyright holder for this preprint (which was not certified by peer review) is the author/funder, who has granted bioRxiv a license to display the preprint in perpetuity. It is made available under aCC-BY-NC-ND 4.0 International license.

References

Akshoomoff, N., Newman, E., Thompson, W. K., McCabe, C., Bloss, C. S., Chang, L., . . . Jernigan, T. L. (2014). The NIH Toolbox Cognition Battery: results from a large normative developmental sample (PING). *Neuropsychology, 28*(1), 1-10. doi:10.1037/neu0000001

Amlien, I. K., Fjell, A. M., Tamnes, C. K., Grydeland, H., Krogsrud, S. K., Chaplin, T. A., . . . Walhovd, K. B. (2016). Organizing Principles of Human Cortical Development--Thickness and Area from 4 to 30 Years: Insights from Comparative Primate Neuroanatomy. *Cereb Cortex, 26*(1), 257-267. doi:10.1093/cercor/bhu214

Andrews, D. S., Avino, T. A., Gudbrandsen, M., Daly, E., Marquand, A., Murphy, C. M., . . . Ecker, C. (2017). In Vivo Evidence of Reduced Integrity of the Gray-White Matter Boundary in Autism Spectrum Disorder. *Cereb Cortex, 27*(2), 877-887. doi:10.1093/cercor/bhw404

Bartzokis, G. (2005). Brain Myelination in Prevalent Neuropsychiatric Developmental Disorders: Primary and Comorbid Addiction. *Adolesc Psychiatry, 29*, 55-96.

Baumann, N., & Pham-Dinh, D. (2001). Biology of oligodendrocyte and myelin in the mammalian central nervous system. *Physiol Rev, 81*(2), 871-927. doi:10.1152/physrev.2001.81.2.871

Blakemore, S. J. (2012). Imaging brain development: the adolescent brain. *Neuroimage, 61*(2), 397-406. doi:10.1016/j.neuroimage.2011.11.080

Brown, T. T., & Jernigan, T. L. (2012). Brain development during the preschool years. *Neuropsychol Rev, 22*(4), 313-333. doi:10.1007/s11065-012-9214-1

Buuren, S. v., & Groothuis-Oudshoorn, K. (2011). mice: Multivariate imputation by chained equations in R. *Journal of Statistical Software, 45*(3), 1-67. doi:http://dx.doi.org/10.18637/jss.v045.i03

Casey, B. J., Tottenham, N., Liston, C., & Durston, S. (2005). Imaging the developing brain: what have we learned about cognitive development? *Trends Cogn Sci, 9*(3), 104-110. doi:10.1016/j.tics.2005.01.011

Deoni, S. C. L., Dean, D. C., 3rd, Remer, J., Dirks, H., & O'Muircheartaigh, J. (2015). Cortical maturation and myelination in healthy toddlers and young children. *Neuroimage, 115*, 147-161. doi:10.1016/j.neuroimage.2015.04.058

Desikan, R. S., Segonne, F., Fischl, B., Quinn, B. T., Dickerson, B. C., Blacker, D., . . . Killiany, R. J. (2006). An automated labeling system for subdividing the human cerebral cortex on MRI scans into gyral based regions of interest. *Neuroimage, 31*(3), 968-980. doi:10.1016/j.neuroimage.2006.01.021

Dougherty, R. F., Ben-Shachar, M., Deutsch, G. K., Hernandez, A., Fox, G. R., & Wandell, B. A. (2007). Temporal-callosal pathway diffusivity predicts phonological skills in children. *Proceedings of the National Academy of Sciences, 104*(20), 8556. doi:10.1073/pnas.0608961104

Esteban, O., Birman, D., Schaer, M., Koyejo, O. O., Poldrack, R. A., & Gorgolewski, K. J. (2017). MRIQC: Advancing the automatic prediction of image quality in MRI from unseen sites. *PLoS One, 12*(9), e0184661. doi:10.1371/journal.pone.0184661

Fischl, B., van der Kouwe, A., Destrieux, C., Halgren, E., Segonne, F., Salat, D. H., . . . Dale, A. M. (2004). Automatically parcellating the human cerebral cortex. *Cereb Cortex, 14*(1), 11-22.

Fukunaga, M., Li, T. Q., van Gelderen, P., de Zwart, J. A., Shmueli, K., Yao, B., . . . Duyn, J. H. (2010). Layer-specific variation of iron content in cerebral cortex as a source of MRI contrast. *Proc Natl Acad Sci U S A, 107*(8), 3834-3839. doi:10.1073/pnas.0911177107

bioRxiv preprint doi: https://doi.org/10.1101/681221; this version posted January 28, 2020. The copyright holder for this preprint (which was not certified by peer review) is the author/funder, who has granted bioRxiv a license to display the preprint in perpetuity. It is made available under aCC-BY-NC-ND 4.0 International license.

Ganzetti, M., Wenderoth, N., & Mantini, D. (2014). Whole brain myelin mapping using T1- and T2-weighted MR imaging data. *Front Hum Neurosci, 8*, 671. doi:10.3389/fnhum.2014.00671

Geschwind, D. H., & Rakic, P. (2013). Cortical evolution: judge the brain by its cover. *Neuron, 80*(3), 633-647. doi:10.1016/j.neuron.2013.10.045

Glasser, M. F., Sotiropoulos, S. N., Wilson, J. A., Coalson, T. S., Fischl, B., Andersson, J. L., . . . Jenkinson, M. (2013). The minimal preprocessing pipelines for the Human Connectome Project. *NeuroImage, 80*, 105-124. doi:https://doi.org/10.1016/j.neuroimage.2013.04.127

Glasser, M. F., & Van Essen, D. C. (2011). Mapping human cortical areas in vivo based on myelin content as revealed by T1- and T2-weighted MRI. *J Neurosci, 31*(32), 11597-11616. doi:10.1523/jneurosci.2180-11.2011

Grydeland, H., Vertes, P. E., Vasa, F., Romero-Garcia, R., Whitaker, K., Alexander-Bloch, A. F., . . . Bullmore, E. T. (2019). Waves of Maturation and Senescence in Micro-structural MRI Markers of Human Cortical Myelination over the Lifespan. *Cereb Cortex, 29*(3), 1369-1381. doi:10.1093/cercor/bhy330

Grydeland, H., Walhovd, K. B., Tamnes, C. K., Westlye, L. T., & Fjell, A. M. (2013). Intracortical Myelin Links with Performance Variability across the Human Lifespan: Results from T1- and T2-Weighted MRI Myelin Mapping and Diffusion Tensor Imaging. *33*(47), 18618-18630. doi:10.1523/JNEUROSCI.2811-13.2013 %J The Journal of Neuroscience

Grydeland, H., Westlye, L. T., Walhovd, K. B., & Fjell, A. M. (2016). Intracortical Posterior Cingulate Myelin Content Relates to Error Processing: Results from T1- and T2-Weighted MRI Myelin Mapping and Electrophysiology in Healthy Adults. *Cereb Cortex, 26*(6), 2402-2410. doi:10.1093/cercor/bhv065

Hagiwara, A., Hori, M., Kamagata, K., Warntjes, M., Matsuyoshi, D., Nakazawa, M., . . . Aoki, S. (2018). Myelin Measurement: Comparison Between Simultaneous Tissue Relaxometry, Magnetization Transfer Saturation Index, and T1w/T2w Ratio Methods. *Scientific Reports, 8*(1), 10554. doi:10.1038/s41598-018-28852-6

Huber, E., Henriques, R. N., Owen, J. P., Rokem, A., & Yeatman, J. D. (2019). Applying microstructural models to understand the role of white matter in cognitive development. *Dev Cogn Neurosci, 36*, 100624. doi:https://doi.org/10.1016/j.dcn.2019.100624

Insel, T. R. (2010). Rethinking schizophrenia. *Nature, 468*(7321), 187-193. doi:10.1038/nature09552

Jernigan, T. L., Brown, T. T., Hagler, D. J., Akshoomoff, N., Bartsch, H., Newman, E., . . . Dale, A. M. (2016). The Pediatric Imaging, Neurocognition, and Genetics (PING) Data Repository. *Neuroimage, 124*, 1149-1154. doi:https://doi.org/10.1016/j.neuroimage.2015.04.057

Khundrakpam, B. S., Lewis, J. D., Jeon, S., Kostopoulos, P., Ituria Medina, Y., Chouinard-Decorte, F., & Evans, A. C. (2019). Exploring Individual Brain Variability during Development based on Patterns of Maturational Coupling of Cortical Thickness: A Longitudinal MRI Study. *Cereb Cortex, 29*(1), 178-188. doi:10.1093/cercor/bhx317

Koenig, S. H. (1991). Cholesterol of myelin is the determinant of gray-white contrast in MRI of brain. *Magn Reson Med, 20*(2), 285-291.

Kremen, W. S., Fennema-Notestine, C., Eyler, L. T., Panizzon, M. S., Chen, C. H., Franz, C. E., . . . Dale, A. M. (2013). Genetics of brain structure: contributions from the Vietnam Era Twin Study of Aging. *Am J Med Genet B Neuropsychiatr Genet, 162b*(7), 751-761. doi:10.1002/ajmg.b.32162

bioRxiv preprint doi: https://doi.org/10.1101/681221; this version posted January 28, 2020. The copyright holder for this preprint (which was not certified by peer review) is the author/funder, who has granted bioRxiv a license to display the preprint in perpetuity. It is made available under aCC-BY-NC-ND 4.0 International license.

Lebel, C., & Deoni, S. (2018). The development of brain white matter microstructure. *Neuroimage, 182*, 207-218. doi:10.1016/j.neuroimage.2017.12.097

Lewis, J. D., Evans, A. C., & Tohka, J. (2018). T1 white/gray contrast as a predictor of chronological age, and an index of cognitive performance. *Neuroimage, 173*, 341-350. doi:10.1016/j.neuroimage.2018.02.050

Lewis, J. D., Fonov, V. S., Collins, D. L., Evans, A. C., & Tohka, J. (2019). Cortical and subcortical T1 white/gray contrast, chronological age, and cognitive performance. *NeuroImage, 196*, 276-288. doi:10.1016/j.neuroimage.2019.04.022

Liu, S., Li, A., Zhu, M., Li, J., & Liu, B. (2019). Genetic influences on cortical myelination in the human brain. *Genes Brain Behav, 18*(4), e12537. doi:10.1111/gbb.12537

Miller, D. J., Duka, T., Stimpson, C. D., Schapiro, S. J., Baze, W. B., McArthur, M. J., . . . Sherwood, C. C. (2012). Prolonged myelination in human neocortical evolution. *Proc Natl Acad Sci U S A, 109*(41), 16480-16485. doi:10.1073/pnas.1117943109

Miot-Noirault, E., Barantin, L., Akoka, S., & Le Pape, A. (1997). T2 relaxation time as a marker of brain myelination: experimental MR study in two neonatal animal models. *J Neurosci Methods, 72*(1), 5-14.

Nakamura, K., Chen, J. T., Ontaneda, D., Fox, R. J., & Trapp, B. D. (2017). T1-/T2-weighted ratio differs in demyelinated cortex in multiple sclerosis. *Ann Neurol, 82*(4), 635-639. doi:10.1002/ana.25019

Nieuwenhuys, R. (2013). The myeloarchitectonic studies on the human cerebral cortex of the Vogt-Vogt school, and their significance for the interpretation of functional neuroimaging data. *Brain Struct Funct, 218*(2), 303-352. doi:10.1007/s00429-012-0460-z

Norbom, L. B., Doan, N. T., Alnaes, D., Kaufmann, T., Moberget, T., Rokicki, J., . . . Tamnes, C. K. (2019). Probing Brain Developmental Patterns of Myelination and Associations With Psychopathology in Youths Using Gray/White Matter Contrast. *Biol Psychiatry, 85*(5), 389-398. doi:10.1016/j.biopsych.2018.09.027

Ritchie, J., Pantazatos, S. P., & French, L. (2018). Transcriptomic characterization of MRI contrast with focus on the T1-w/T2-w ratio in the cerebral cortex. *Neuroimage, 174*, 504-517. doi:10.1016/j.neuroimage.2018.03.027

Salat, D. H., Lee, S. Y., van der Kouwe, A. J., Greve, D. N., Fischl, B., & Rosas, H. D. (2009). Age-associated alterations in cortical gray and white matter signal intensity and gray to white matter contrast. *Neuroimage, 48*(1), 21-28. doi:10.1016/j.neuroimage.2009.06.074

Shafee, R., Buckner, R. L., & Fischl, B. (2015). Gray matter myelination of 1555 human brains using partial volume corrected MRI images. *Neuroimage, 105*, 473-485. doi:10.1016/j.neuroimage.2014.10.054

Smith, S. M., & Nichols, T. E. (2009). Threshold-free cluster enhancement: addressing problems of smoothing, threshold dependence and localisation in cluster inference. *NeuroImage, 44*(1), 83-98. doi:10.1016/j.neuroimage.2008.03.061

Snaidero, N., & Simons, M. (2017). The logistics of myelin biogenesis in the central nervous system. *Glia, 65*(7), 1021-1031. doi:10.1002/glia.23116

Tamnes, C. K., Herting, M. M., Goddings, A. L., Meuwese, R., Blakemore, S. J., Dahl, R. E., . . . Mills, K. L. (2017). Development of the Cerebral Cortex across Adolescence: A Multisample Study of Inter-Related Longitudinal Changes in Cortical Volume, Surface Area, and Thickness. *J Neurosci, 37*(12), 3402-3412. doi:10.1523/jneurosci.3302-16.2017

Travis, K. E., Adams, J. N., Kovachy, V. N., Ben-Shachar, M., & Feldman, H. M. (2017). White matter properties differ in 6-year old Readers and Pre-readers. *Brain Struct Funct, 222*(4), 1685-1703. doi:10.1007/s00429-016-1302-1

bioRxiv preprint doi: https://doi.org/10.1101/681221; this version posted January 28, 2020. The copyright holder for this preprint (which was not certified by peer review) is the author/funder, who has granted bioRxiv a license to display the preprint in perpetuity. It is made available under aCC-BY-NC-ND 4.0 International license.

Uddin, M. N., Figley, T. D., Solar, K. G., Shatil, A. S., & Figley, C. R. (2019). Comparisons between multi-component myelin water fraction, T1w/T2w ratio, and diffusion tensor imaging measures in healthy human brain structures. *Scientific Reports, 9*(1), 2500. doi:10.1038/s41598-019-39199-x

Van Essen, D. C., & Glasser, M. F. (2014). In vivo architectonics: a cortico-centric perspective. *NeuroImage, 93 Pt 2*, 157-164. doi:10.1016/j.neuroimage.2013.04.095

Vandewouw, M. M., Young, J. M., Shroff, M. M., Taylor, M. J., & Sled, J. G. (2019). Altered myelin maturation in four year old children born very preterm. *Neuroimage Clin, 21*, 101635. doi:10.1016/j.nicl.2018.101635

Vijayakumar, N., Allen, N. B., Youssef, G., Dennison, M., Yucel, M., Simmons, J. G., & Whittle, S. (2016). Brain development during adolescence: A mixed-longitudinal investigation of cortical thickness, surface area, and volume. *Hum Brain Mapp, 37*(6), 2027-2038. doi:10.1002/hbm.23154

Waxman, S. G., & Bennett, M. V. (1972). Relative conduction velocities of small myelinated and non-myelinated fibres in the central nervous system. *Nat New Biol, 238*(85), 217-219.

Weintraub, S., Bauer, P. J., Zelazo, P. D., Wallner-Allen, K., Dikmen, S. S., Heaton, R. K., . . . Gershon, R. C. (2013). I. NIH Toolbox Cognition Battery (CB): introduction and pediatric data. *Monogr Soc Res Child Dev, 78*(4), 1-15. doi:10.1111/mono.12031

Weintraub, S., Dikmen, S. S., Heaton, R. K., Tulsky, D. S., Zelazo, P. D., Bauer, P. J., . . . Gershon, R. C. (2013). Cognition assessment using the NIH Toolbox. *Neurology, 80*(11 Suppl 3), S54-64. doi:10.1212/WNL.0b013e3182872ded

Westlye, L. T., Walhovd, K. B., Dale, A. M., Bjornerud, A., Due-Tonnessen, P., Engvig, A., . . . Fjell, A. M. (2010). Differentiating maturational and aging-related changes of the cerebral cortex by use of thickness and signal intensity. *Neuroimage, 52*(1), 172-185. doi:10.1016/j.neuroimage.2010.03.056

White, N., Roddey, C., Shankaranarayanan, A., Han, E., Rettmann, D., Santos, J., . . . Dale, A. (2010). PROMO: Real-time prospective motion correction in MRI using image-based tracking. *Magn Reson Med, 63*(1), 91-105. doi:10.1002/mrm.22176

Wickham, H. (2009). *ggplot2 Elegant Graphics for Data Analysis* (1 ed.): Springer-Verlag New York.

Wierenga, L. M., Bos, M. G. N., van Rossenberg, F., & Crone, E. A. (2019). Sex Effects on Development of Brain Structure and Executive Functions: Greater Variance than Mean Effects. *J Cogn Neurosci, 31*(5), 730-753. doi:10.1162/jocn_a_01375

Winkler, A. M., Ridgway, G. R., Webster, M. A., Smith, S. M., & Nichols, T. E. (2014). Permutation inference for the general linear model. *NeuroImage, 92*, 381-397. doi:10.1016/j.neuroimage.2014.01.060

Yakovlev, P. A., & Lecours, I. R. (1967). The myelogenetic cycles of regional maturation of the brain. In A. Minkowski (Ed.), *Regional Development of the brain in early life.* (pp. 3-70). Oxford: Blackwell.

Ziegler, G., Hauser, T. U., Moutoussis, M., Bullmore, E. T., Goodyer, I. M., Fonagy, P., . . . Consortium, N. (2019). Compulsivity and impulsivity traits linked to attenuated developmental frontostriatal myelination trajectories. *Nature Neuroscience*. doi:10.1038/s41593-019-0394-3

bioRxiv preprint doi: https://doi.org/10.1101/681221; this version posted January 28, 2020. The copyright holder for this preprint (which was not certified by peer review) is the author/funder, who has granted bioRxiv a license to display the preprint in perpetuity. It is made available under aCC-BY-NC-ND 4.0 International license.

	MRI sample	**Cognition sample**
N	621	611
Age (years)	3.2-21.0 (mean= 12.4, SD= 4.8)	3.2-21.0 (mean= 12.5, SD= 4.8)
Sex	Boys= 318, Girls = 303	Boys=310, Girls = 301
Self-reported Ethnicity	Hispanic/Latino = 140 Pacific Islander = 5 Asian = 88 African American = 102 Native American = 31 White = 426	Hispanic/Latino = 136 Pacific Islander = 4 Asian = 86 African American = 100 Native American= 31 White = 420
Handedness	Right handed= 532 Left handed= 60 Mixed =24 Not established = 3 Not available = 2	Right handed = 523 Left handed= 60 Mixed = 24 Not established = 3 Not available = 1
Ever diagnosed with ADHD	Yes = 48 No = 567 Not available = 6	Yes = 48 No = 557 Not available = 6

Table1. Sample demographics. The table shows sample demographics for the MRI sample and the cognition sample. The total ethnicity numbers exceed total sample size as several subjects identified as belonging to more than one ethnicity group.

bioRxiv preprint doi: https://doi.org/10.1101/681221; this version posted January 28, 2020. The copyright holder for this preprint (which was not certified by peer review) is the author/funder, who has granted bioRxiv a license to display the preprint in perpetuity. It is made available under aCC-BY-NC-ND 4.0 International license.

Test	**Cognitive Ability**	**Abbreviation**
Dimensional Change Card Sort Test	Cognitive flexibility	Cognitive flexibility
Flanker Inhibitory Control and Attention Test	Inhibitory control	Inhibition
	Visual attention	Attention
Picture Sequence Memory Test	Episodic memory	Episodic memory
Pattern Comparison Processing Speed Test	Processing speed	Processing speed
Oral Reading Recognition Test	Oral reading skill	Reading
List Sorting Working Memory Test	Working memory	Working memory
Picture Vocabulary Test	Vocabulary knowledge	Vocabulary

Table 2. Overview of the NIH Toolbox Cognition Battery measures. The table shows the tests in order as presented to subjects, the cognitive abilities assessed, and the abbreviations used in the current paper.

Cortical region	**Age effect (t)**	**Age-Sex interaction**	**General cognitive ability effect**

bioRxiv preprint doi: https://doi.org/10.1101/681221; this version posted January 28, 2020. The copyright holder for this preprint (which was not certified by peer review) is the author/funder, who has granted bioRxiv a license to display the preprint in perpetuity. It is made available under aCC-BY-NC-ND 4.0 International license.

			effect (t)		**(t)**	
	LH	RH	LH	RH	LH	RH
Banks superior temporal sulcus	10.5	8.6	2.4	2.1	-2.0	-2.0
Caudal anterior cingulate	8.6	9.2	2.4	2.6	-2.3	-1.9
Caudal middle frontal	14.4	13.4	3.0	2.3	-3.1	-2.4
Cuneus	5.5	3.9	1.7	1.2	-1.3	-1.2
Entorhinal	7.9	5.7	1.9	1.1	-1.9	-1.1
Fusiform	8.2	7.0	1.8	1.1	-1.5	-1.1
Inferior parietal	10.3	9.4	3.1	2.9	-2.0	-2.6
Inferior temporal	8.5	6.8	2.1	1.3	-1.7	-1.6
Isthmus cingulate	8.8	8.8	1.2	1.0	-1.5	-1.4
Lateral occipital	6.3	6.2	2.0	2.1	-1.4	-1.9
Lateral orbitofrontal	11.4	11.9	3.2	2.3	-2.8	-1.8
Lingual	6.0	5.8	1.4	1.3	-1.3	-1.1
Medial orbitofrontal	10.7	10.9	2.8	2.9	-1.9	-1.7
Middle temporal	10.5	7.7	2.5	1.6	-2.3	-2.4
Parahippocampal	6.3	5.9	1.2	1.1	-1.1	-0.4
Paracentral	12.4	13.0	2.3	2.4	-2.6	-2.3
Pars opercularis	12.6	10.8	3.1	1.5	-3.1	-2.3
Pars orbitalis	13.0	12.6	3.8	2.4	-3.4	-2.7
Pars triangularis	13.0	12.3	3.4	2.3	-3.3	-2.5
Pericalcarine	3.6	2.9	2.1	2.1	-1.7	-1.3
Postcentral	13.0	10.9	2.5	2.3	-2.9	-2.4
Posterior cingulate	8.9	9.1	1.8	1.8	-2.1	-1.9
Precentral	14.6	13.3	2.7	2.2	-3.0	-2.6
Precuneus	9.7	9.7	2.4	2.2	-2.0	-2.0

bioRxiv preprint doi: https://doi.org/10.1101/681221; this version posted January 28, 2020. The copyright holder for this preprint (which was not certified by peer review) is the author/funder, who has granted bioRxiv a license to display the preprint in perpetuity. It is made available under aCC-BY-NC-ND 4.0 International license.

Rostral anterior cingulate	9.2	9.7	2.7	3.0	-2.0	-1.9
Rostral middle frontal	12.9	13.4	3.7	3.2	-2.9	-2.5
Superior frontal	12.4	12.6	3.3	3.3	-2.5	-2.3
Superior parietal	11.0	10.6	2.8	2.6	-2.2	-2.4
Superior temporal	11.1	7.6	2.4	1.4	-2.6	-2.1
Supramarginal	12.3	10.0	2.7	2.5	-2.4	-2.6
Frontal pole	11.0	12.5	3.4	3.7	-2.0	-2.5
Temporal pole	7.8	6.7	2.4	1.1	-3.3	-2.0
Transverse temporal	12.2	10.1	1.2	0.8	-2.4	-1.7
Insula	8.5	6.0	1.8	0.9	-2.7	-1.6

Table 3. ROI based mean t-statistic of T1w/T2w ratio associations. The table shows each of the 34 ROIs, and the mean t-statistic within each region for the association between T1w/T2w ratio and age, age*sex and general cognitive ability within left and right hemisphere separately.

bioRxiv preprint doi: https://doi.org/10.1101/681221; this version posted January 28, 2020. The copyright holder for this preprint (which was not certified by peer review) is the author/funder, who has granted bioRxiv a license to display the preprint in perpetuity. It is made available under aCC-BY-NC-ND 4.0 International license.

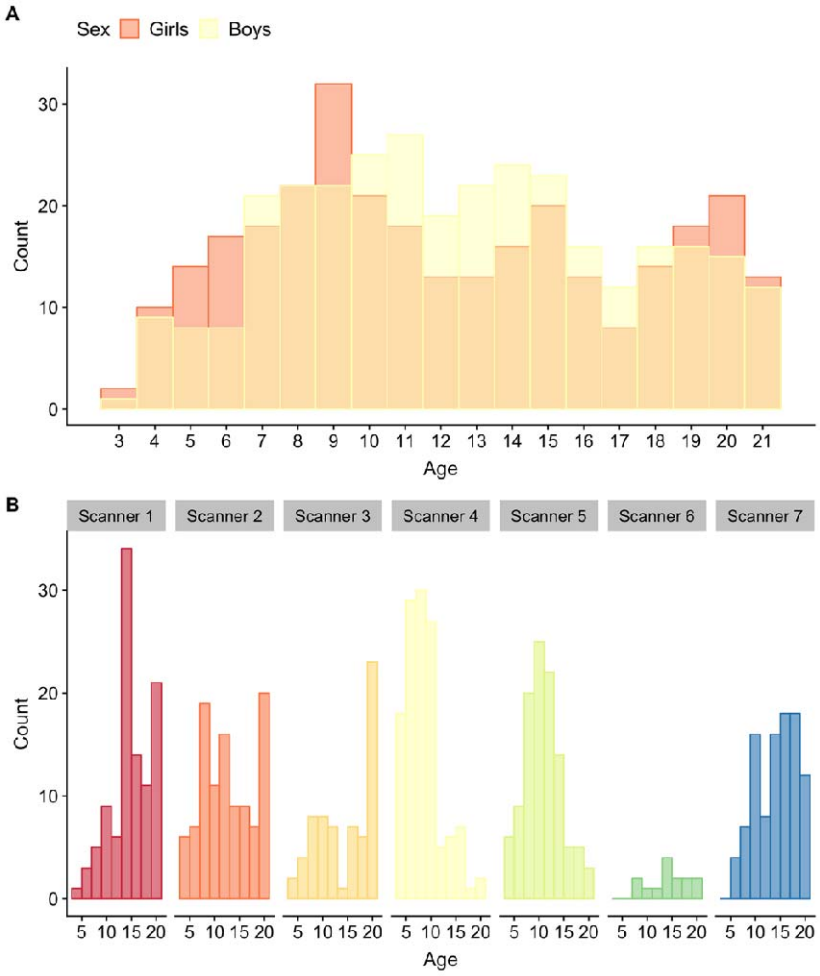

Figure 1. Age and sex distribution for the full MRI sample (n= 621). (A) Depicts the age and sex distribution of the full MRI sample, while (B) depicts the age distribution within each scanner.

bioRxiv preprint doi: https://doi.org/10.1101/681221; this version posted January 28, 2020. The copyright holder for this preprint (which was not certified by peer review) is the author/funder, who has granted bioRxiv a license to display the preprint in perpetuity. It is made available under aCC-BY-NC-ND 4.0 International license.

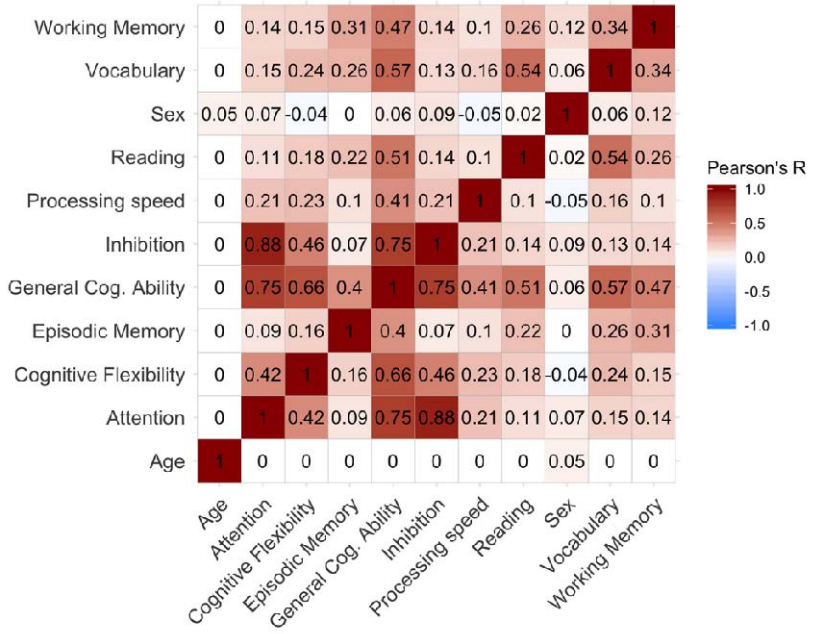

Figure 2. Correlation matrix for age, sex and cognition. The figure depicts Pearson's correlation coefficients for age, sex, general cognitive ability (General Cog. Ability), and individual cognitive sum scores. Warm colors represent positive correlations, while cold colors represent negative correlations. Sum scores, and by extension general cognitive ability, are residualized by linear and quadratic age.

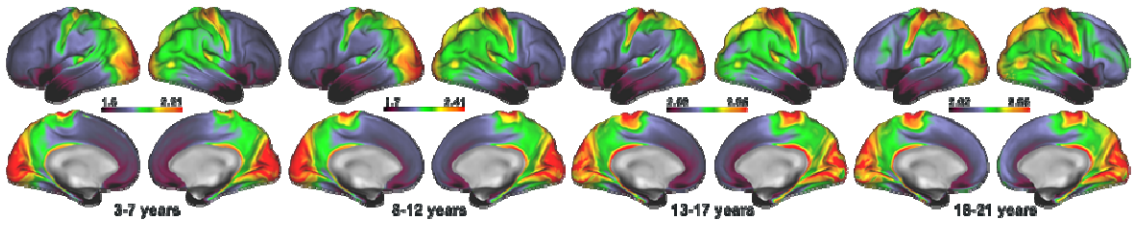

Figure 3. Age binned mean T1w/T2w ratio maps. The figure depicts mean T1w/T2w ratio maps from the full MRI sample (n= 621), devided into 4 age bins of 3-7 years (n= 120), 8-12 years (n= 219), 13-17 years (n= 168), and 18-21 years (n= 114). Warm colors represent regions with higher T1w/T2w ratio, while cold colors represent regions with lower T1w/T2w ratio.

bioRxiv preprint doi: https://doi.org/10.1101/681221; this version posted January 28, 2020. The copyright holder for this preprint (which was not certified by peer review) is the author/funder, who has granted bioRxiv a license to display the preprint in perpetuity. It is made available under aCC-BY-NC-ND 4.0 International license.

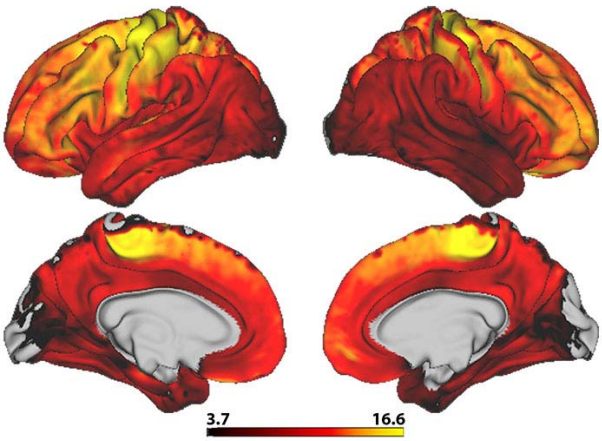

Figure 4. Vertex-wise associations between T1w/T2w ratio and age. The figure depicts the t statistics map, masked by familywise error - across contrast corrected p values threasholded at a minimum $-\log_p$ of 1.6 to correct for both hemispheres. Warm colors represent a postive age association.

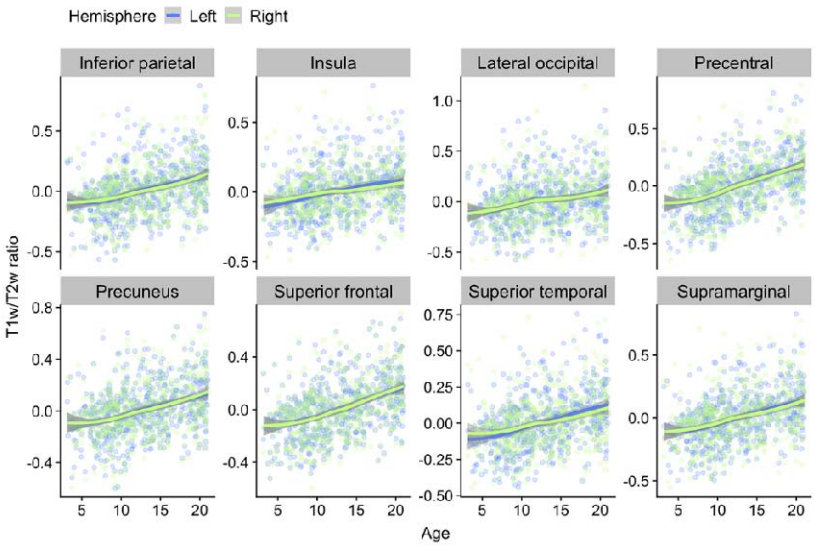

Figure 5. Regional loess visualizations of associations between T1w/T2w ratio and age. The plots show age plotted against mean T1w/T2w ratio within a selection of regions from different cortical lobes. Datapoints and smooth splines are color coded by hemisphere. T1w/T2w ratio values are residualized by sex and scanner.

bioRxiv preprint doi: https://doi.org/10.1101/681221; this version posted January 28, 2020. The copyright holder for this preprint (which was not certified by peer review) is the author/funder, who has granted bioRxiv a license to display the preprint in perpetuity. It is made available under aCC-BY-NC-ND 4.0 International license.

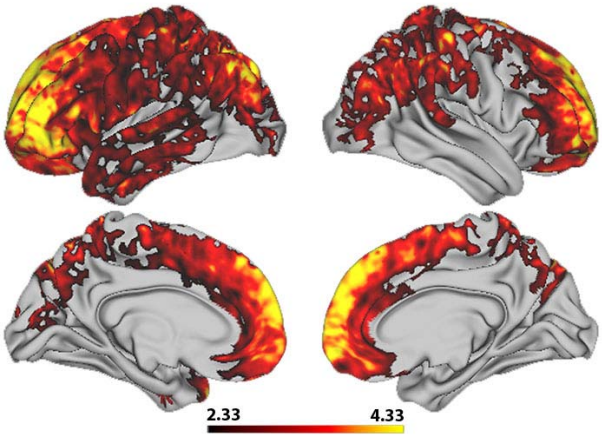

Figure 6. Vertex-wise associations between T1w/T2w ratio and the interaction between age and sex. The figure depicts the t statistics map, masked by familywise error - across contrast corrected p values threasholded at a minimum $-\log_p$ of 1.6 to correct for both hemispheres. Warm colors represent a postive interaction effect.

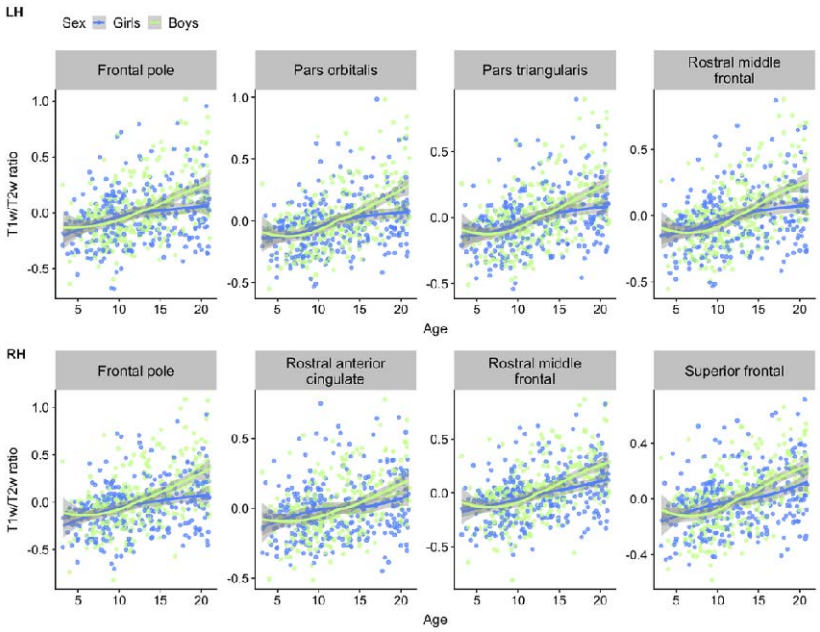

Figure 7. Visualizations of T1w/T2w ratio versus age color coded for sex. The plots shows age plotted against mean T1w/T2w ratio within frontal regions, chosen based on the highest regional age*sex mean t-statistics, with datapoints and smooth splines color coded by sex. T1w/T2w ratio values are residualized by scanner.

bioRxiv preprint doi: https://doi.org/10.1101/681221; this version posted January 28, 2020. The copyright holder for this preprint (which was not certified by peer review) is the author/funder, who has granted bioRxiv a license to display the preprint in perpetuity. It is made available under aCC-BY-NC-ND 4.0 International license.

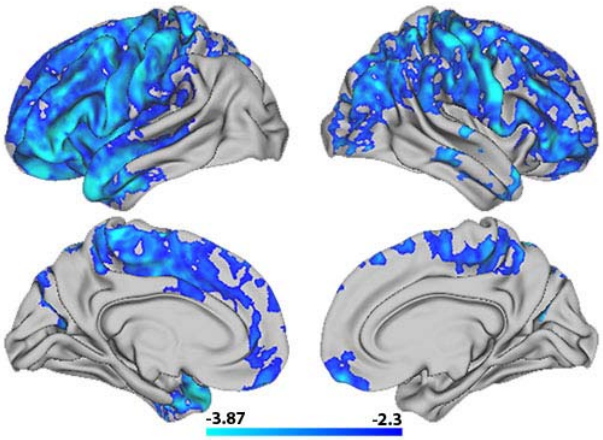

Figure 8. Vertex-wise associations between T1w/T2w ratio and general cogntive ability. The figure depicts the t statistics map, masked by familywise error - across contrast corrected p values threasholded at a minimum $-\log_p$ of 1.6 to correct for both hemispheres. Cold colors represent a negative association between T1w/T2w ratio and general cogntive ability.

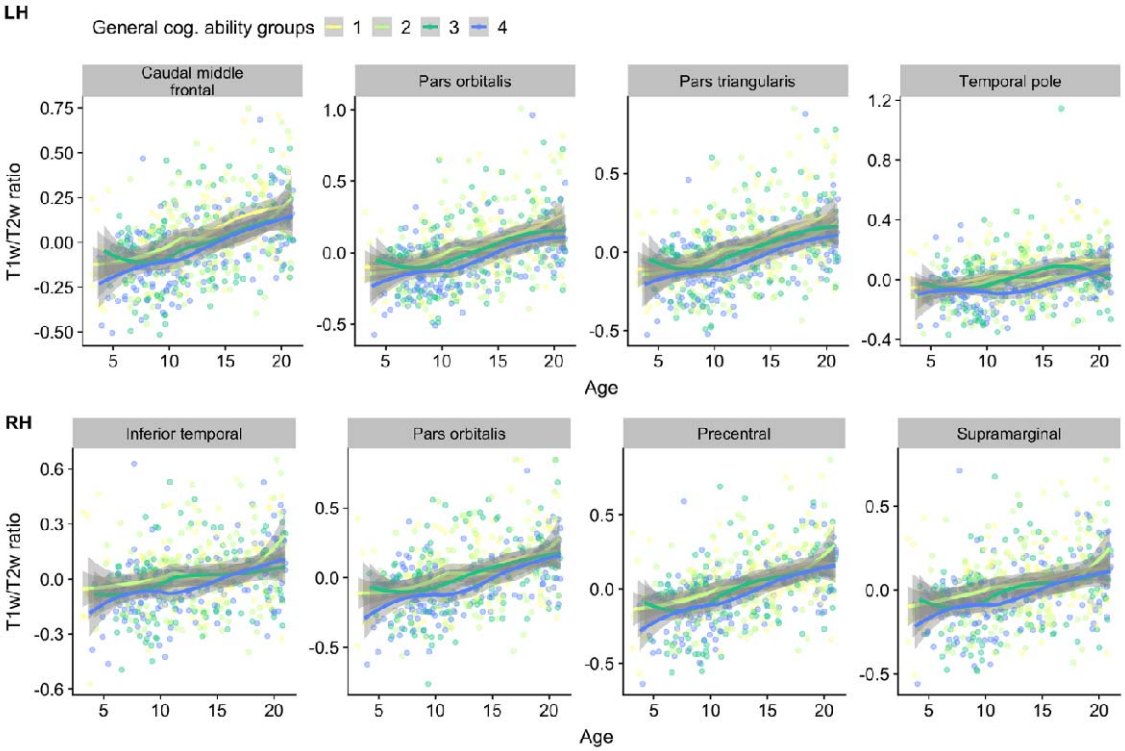

Figure 9. Visualizations of T1w/T2w ratio versus age, color coded by general cognitive ability. The plots depict age plotted against mean T1w/T2w ratio within frontal regions, chosen based on the the

bioRxiv preprint doi: https://doi.org/10.1101/681221; this version posted January 28, 2020. The copyright holder for this preprint (which was not certified by peer review) is the author/funder, who has granted bioRxiv a license to display the preprint in perpetuity. It is made available under aCC-BY-NC-ND 4.0 International license.

highest regional mean t-statistics, with data points and smooth splines color coded by general cogntive ability, resulting in 4 equal qunatiles with worst (yellow) to best (blue) cognitive performers. T1w/T2w ratio is sex and scanner residualized, while general cognitive performance is residualized by linear and quadratic age.

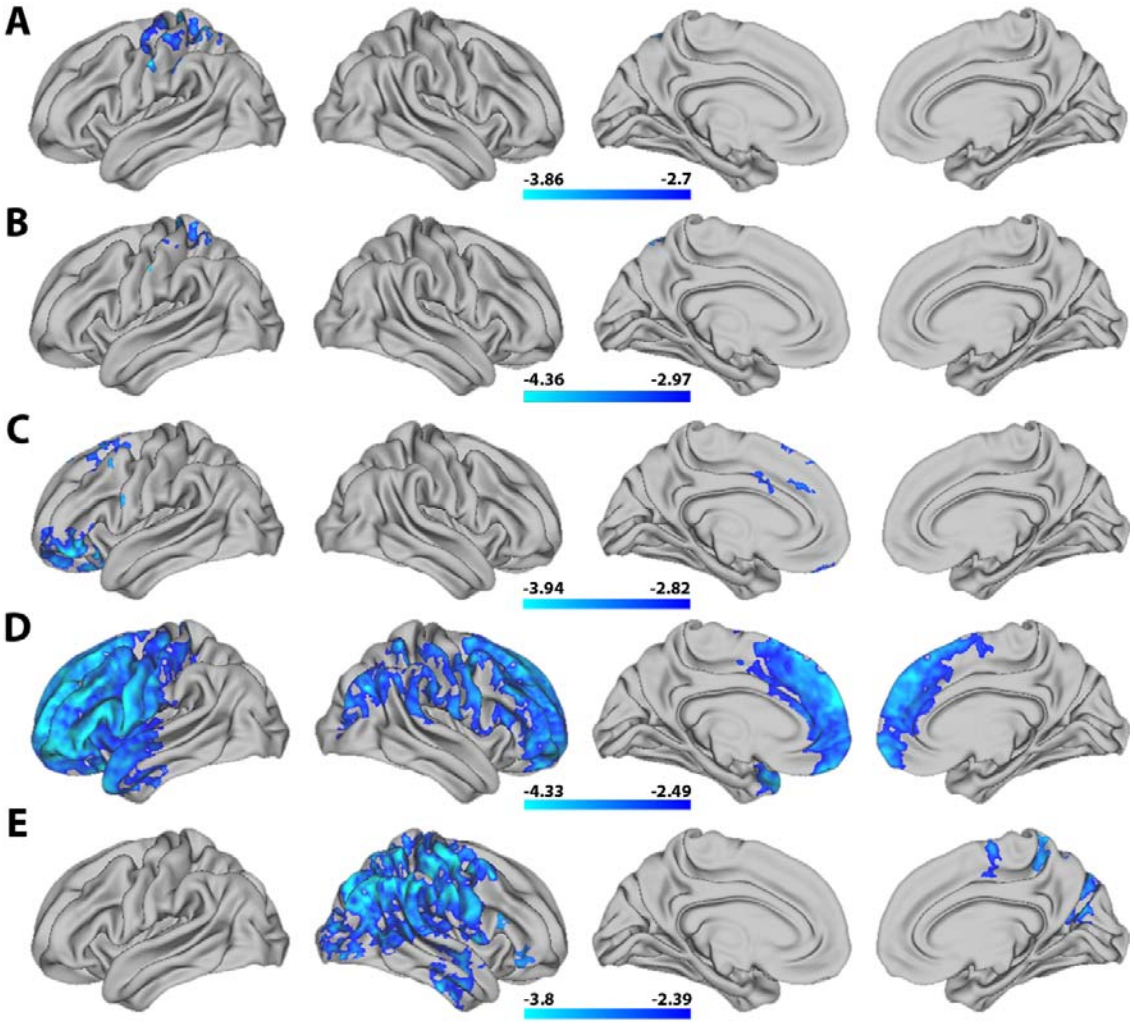

Figure 10. Vertex-wise associations between T1w/T2w ratio and individual cognitive sum scores. The figure depicts t statistics maps from top to bottom for (A) inhibition, (B) attention, (C) vocabulary, (D) reading, and (E) working memory. The maps are masked by familywise error - across contrast corrected p values threasholded at a minimum $-\log_p$ of 1.6 to correct for both hemispheres. Cold colors represent a negative association between T1w/T2w ratio and each sum score.

bioRxiv preprint doi: https://doi.org/10.1101/681221; this version posted January 28, 2020. The copyright holder for this preprint (which was not certified by peer review) is the author/funder, who has granted bioRxiv a license to display the preprint in perpetuity. It is made available under aCC-BY-NC-ND 4.0 International license.